

2020-01

Global trends in water and sediment fluxes of the world's large rivers

Li, L

<http://hdl.handle.net/10026.1/17670>

10.1016/j.scib.2019.09.012

Science Bulletin

Elsevier BV

All content in PEARL is protected by copyright law. Author manuscripts are made available in accordance with publisher policies. Please cite only the published version using the details provided on the item record or document. In the absence of an open licence (e.g. Creative Commons), permissions for further reuse of content should be sought from the publisher or author.

Article

Global trends in water and sediment fluxes of the world's large rivers

Li Li, Jinren Ni, Fang Chang, Yao Yue, Natalia Frolova, Dmitry Magritsky, Alistair G.L. Borthwick, Philippe Ciais, Yichu Wang, Chunmiao Zheng, Desmond E. Walling

PII: S2095-9273(19)30553-5
DOI: <https://doi.org/10.1016/j.scib.2019.09.012>
Reference: SCIB 823

To appear in: *Science Bulletin*

Received Date: 1 August 2019
Revised Date: 16 August 2019
Accepted Date: 19 August 2019

Please cite this article as: L. Li, J. Ni, F. Chang, Y. Yue, N. Frolova, D. Magritsky, A.G.L. Borthwick, P. Ciais, Y. Wang, C. Zheng, D.E. Walling, Global trends in water and sediment fluxes of the world's large rivers, *Science Bulletin* (2019), doi: <https://doi.org/10.1016/j.scib.2019.09.012>

This is a PDF file of an article that has undergone enhancements after acceptance, such as the addition of a cover page and metadata, and formatting for readability, but it is not yet the definitive version of record. This version will undergo additional copyediting, typesetting and review before it is published in its final form, but we are providing this version to give early visibility of the article. Please note that, during the production process, errors may be discovered which could affect the content, and all legal disclaimers that apply to the journal pertain.



Title: Global trends in water and sediment fluxes of the world's large rivers

Authors: Li Li^a, Jinren Ni^{a*}, Fang Chang^a, Yao Yue^b, Natalia Frolova^c, Dmitry
5 Magritsky^c, Alistair G. L. Borthwick^d, Philippe Ciais^e, Yichu Wang^{a, f}, Chunmiao
Zheng^g, Desmond E. Walling^h

Affiliations:

^aKey Laboratory of Water and Sediment Sciences, Ministry of Education; College of
10 Environmental Sciences and Engineering, Peking University, Beijing 100871, China.

^bState Key Laboratory of Water Resources and Hydropower Engineering Science,
School of Water Resources and Hydropower Engineering, Wuhan University, Wuhan
430072, China.

^cDepartment of Hydrology, Faculty of Geography, Moscow State University, Moscow
15 119991, Russia.

^dInstitute of Infrastructure and Environment, School of Engineering, the University of
Edinburgh, the King's Buildings, Edinburgh EH9 3JL, UK.

^eLaboratoire des Sciences du Climat et de l'Environnement, IPSL, CEA, CNRS,
UVSQ, 91191 Gif-sur-Yvette, France.

20 ^fBeijing Innovation Center-Engineering Science & Advanced Technology, Peking
University, Beijing 100871, China.

^gSchool of Environmental Science and Engineering, Southern University of Science
and Technology, Shenzhen 518055, China.

^hDepartment of Geography, College of Life and Environmental Sciences, University
25 of Exeter, Exeter, EX4 4RJ, UK.

* **Corresponding author:** Email: jinrenni@pku.edu.cn

Received 2019-08-01, received in revised form 2019-08-16, accepted 2019-08-19

Abstract

Water and sediment transport from rivers to oceans is of primary importance in global
5 geochemical cycle. Against the background of global change, this study examines the
changes in water and sediment fluxes and their drivers for 4,307 large rivers
worldwide (basin area $\geq 1,000 \text{ km}^2$) based on the longest available records. Here we
find that 24% of the world's large rivers experienced significant changes in water flux
and 40% in sediment flux, most notably declining trends in water and sediment fluxes
10 in Asia's large rivers and an increasing trend in suspended sediment concentrations in
the Amazon River. In particular, nine binary patterns of changes in water-sediment
fluxes are interpreted in terms of climate change and human impacts. The change of
precipitation is found significantly correlated to the change of water flux in 71% of
the world's large rivers, while dam operation and irrigation rather control the change
15 of sediment flux in intensively managed catchments. Globally, the annual water flux
from rivers to sea of the recent years remained stable compared with the long-time
average annual value, while the sediment flux has decreased by 20.8%.

Key words: water and sediment, global trend, co-varying pattern, cause, large river

1. Introduction

Changing fluvial water and sediment fluxes exert a key effect on river ecosystems [1, 2] and their management [3]. Such changes represent critical aspects of global change [4], also affecting delta evolution and sustainability [5, 6] and aquatic organisms' habitats [7–9]. Much literature currently exists on the separate trends in water or sediment flux associated with individual rivers [5] or groups of rivers [10, 11] due to the limited availability of long-term observational data [12] for coupled records on both water and sediment, particularly for developing countries [13–15]. Walling and Fang [13] analyzed trends of water and sediment fluxes before the 1990s, but their analysis did not extend to rivers in South America, Africa and Oceania. To reveal the rare investigated co-varying trends in addition to the recent trends of water and sediment fluxes in world's large rivers, we compiled long-term records of annual water flux (discharge Q) from 8,089 gauging stations located in 4,307 rivers (all with a basin area $\geq 1,000 \text{ km}^2$), with roughly one fourth of the gauge stations being at the mouth of rivers (Supplementary Data S1 online). The longest record dates from 1806 for the Dresden Station on the Elbe River, and about half of the stations provided records of annual water flux spanning 40 years or more. Information on annual mean suspended sediment concentration (C_{ss}) and annual suspended sediment flux (Q_{ss}) was also collected for 309 of the rivers (516 stations), including stations at the river mouth for 129 rivers (496 stations; Supplementary Data S1 online). The data cover 88% of the land surface, and 60% of the area actively contributing water flux to the oceans [16, 17].

Non-parametric trend analysis based on the longest recorded data series (see Method) was used to identify significant trends in water and sediment fluxes for individual rivers. Furthermore, the co-varying trends under the impacts of climate

change and human activities were presented under a Sudoku framework. It should be noted that the trend analysis requires accounting for the differences in the length of available records to guarantee the reliability and nature of the results. Long duration records can provide more definitive evidence of long-term trends, whereas records covering shorter, more recent periods may provide a clearer indication of contemporary or recent changes. Here, the longest available record for each river was used for trend analysis. Results that compare the magnitude of water flux (Q) and sediment flux (Q_{ss}) in the most recent decade with the longer-term mean are also presented. Based on the reliability analysis on record length in terms of guarantee rate, we suggest that a minimum of 30 years (either continuous or not) is required to reflect the changing trend in a longer period (the recent 40 years, 1971–2010).

2. Materials and Methods

LOADEST [18, 19] was used to evaluate the sediment flux at 123 stations (25% of the 496 stations on the 309 large rivers) using continuously observed daily water flux data and discretely measured sediment flux data on daily based. For each station, the water discharge and suspended sediment concentration time series associated with a given year were used to calibrate regression models that permit the values of daily sediment flux using formulas fitted to the water discharge time series [18]. The Adjusted Maximum Likelihood Estimation (AMLE) method was applied during calibration, and the regression model with lowest Akaike Information Criterion (AIC) value was selected to estimate sediment flux. R^2 values associated with the models fitted to the data from individual stations on the annual basis are presented in Supplementary Data S2 (online).

Trends in Q , C_{SS} , and Q_{SS} were analyzed by means of the non-parametric Mann–Kendall (MK) test [20, 21]. Trend-free pre-whitening (TFPW) was used to ensure data independence before using the MK test [22].

Pre-human sediment fluxes were estimated for the rivers included in the sediment flux database using the Area Relief Temperature sediment delivery model (ART) [23].

Data Sources and detail of Methods were given in Supplementary Information.

3. Results and discussions

3.1 Global trends in water and sediment variations of large rivers

The records of annual water flux (Q) showed no significant change for 3,301 (77%) rivers, decreased significantly for 500 rivers (11%) and increased for 506 rivers (12%) rivers (Fig. 1a). The proportions of rivers experiencing significant changes in Q are highest in Africa and North America (Table S1 online). In Fig. 1a, global distribution map of Q trends is shown with all gauging stations. Stations with decreased Q are mainly located in the central and western Africa, eastern Asia, southern Europe, western North America and eastern Australia. Stations with increased water flux are mainly located in northern Asia, northern Europe, and northern and eastern North America.

Analysis of all the C_{SS} records indicated significant reductions in suspended sediment concentrations for 105 rivers (34%) and an increase in only 22 rivers (7%). The majority of the remaining rivers showed no significant trend (Fig. 1b). Most of rivers with significant changes in C_{SS} are in developing regions (Africa, Asia and South America) (Table S1 online). Rivers with significant decreases in C_{SS} are in eastern Asia and North America, and those with significant increases are in northeastern China, eastern North America and South America.

The majority (82%) of rivers exhibit the trends of the same sign for Q_{ss} and C_{ss} . The sediment flux $Q_{ss} = C_{ss} \times Q$ shows no significant change for 196 (63%) of rivers, with the other 100 (32%) recorded decreases in Q_{ss} . An increased sediment flux is only observed for 13 (4%) of rivers (Fig. 1c). 72% of rivers in Asia show significant upward or downward trends in Q_{ss} , and less than 20% (Table S1 online) in North America and Oceania. Stations with decreasing trends in Q_{ss} are widely distributed in North America and Eastern Asia. Increased Q_{ss} is mostly evident in the Northeastern China and the north of South America.

3.2 Basic patterns for water-sediment co-varying trends and their causes

Figure 2a divides the trends in $[Q, Q_{ss}]$ combination across all rivers into a matrix of nine basic patterns, each according to whether the variable is in stable, decreasing, or increasing. The histogram shows that water and sediment fluxes measured at 138 (45%) rivers belong to Pattern I, with no significant trend in both fluxes. The Pattern II trend of stable Q and decreasing Q_{ss} covers 50 (16%) rivers, and the Pattern V trend of both decreasing Q and Q_{ss} covers 41 (13%) rivers. Compared to Walling and Fang's study [13] which represented past trends in $[Q, Q_{ss}]$ based on a smaller dataset (only in Europe, Asia, and North America), changes to $[Q, Q_{ss}]$ are evident in the present data, as well as a new trend pattern (decrease in water flux with increase in sediment flux).

In all continents, the dominant $[Q, Q_{ss}]$ pattern of change is Pattern I, except in Asia, which contains a mix of Pattern I, II and V. Rivers exhibiting Pattern II are very common worldwide, except for North America and Africa. Pattern III representing stable Q and increasing Q_{ss} is mainly found in South America and Pattern IV representing decreasing Q and stable Q_{ss} is found in North America and Oceania. Looking globally, Q_{ss} has a general stable or decreasing trend in developed regions,

whereas Patterns III and IX associated with an increasing trend in Q_{ss} occur in developing regions, except Asia. Patterns V mainly occur in Asia and Africa, but Pattern VII representing increasing Q and stable Q_{ss} only predominates in North America and Europe. Trends in water and sediment fluxes are exemplified by the representative large rivers for the nine basic $[Q, Q_{ss}]$ patterns in Fig. 2b, including the famous large rivers such as Amazon River, Rhine River, Mississippi River, Yangtze River, Yellow River, Yana River, and Blue Nile River.

To examine the impacts of Asian rivers undergoing the most intensive human interference in recent decades, we compared the statistical results with and without these rivers. It is found that the number of rivers associated with Pattern I does not change noticeably; instead, occurrences of Patterns V and II reduce by 68% and 48% respectively (Fig. 3a), indicating that the reduction in Q_{ss} is widespread in rapidly developing Asian countries where numerous dams have been constructed in recent years. The long-term effect of human activities on Q_{ss} has been estimated using the Area Relief Temperature sediment delivery model [23] (ART) which can provide a reliable estimate (overall R^2 of the 461 rivers equals 0.99, Table S2 online) of the pre-human sediment flux (i.e. natural sediment flux before there was dominant human disturbance) of a river basin. A comparison of these estimates with the observed long-term mean Q_{ss} in most (71%) large rivers in Asia has decreased compared to pre-human Q_{ss} values (below the 1 : 1 line in Fig. 3b).

Over the recent decade (2000–2010), the $[Q, Q_{ss}]$ trends for global rivers have changed substantially compared to the previous decades. The proportion of rivers showing Pattern I is decreasing, whereas the proportions showing with Patterns II and V are increasing (Fig. 3c). These changes primarily resulted from the great reduction of Q and Q_{ss} (Fig. 3d) in Asian rivers after 2000 owing to dam constructions.

In seeking to establish the key factors responsible for producing the nine different patterns of $[Q, Q_{SS}]$ changes and their global distribution, both climate and human impacts have been identified as important controls. In arid regions, the water discharge data for the majority (81%) of stations demonstrate either a significant decreasing trend, or a decreasing but not statistically significant trend. In humid regions, most stations (71%) show a stable long-term trend. Compared with water flux, C_{SS} seems less sensitive to background climate conditions, but primarily controlled by human activities. When Activity of type A (e.g. dam construction, irrigation and implementation of soil and water conservation programs) is implemented, C_{SS} is significantly reduced. However, Activity of type B (e.g. deforestation, mining, and land clearance) coincides increased C_{SS} , which is particularly common in developing countries.

The trend in Q_{SS} is determined by changes in Q and C_{SS} . Only 59% of stations have consistent trends in both Q_{SS} and Q , whereas 82% have consistent trends in Q_{SS} and C_{SS} . This suggests that C_{SS} is the dominant factor explaining changes of Q_{SS} . However, changing Q also plays a role, and thus the trends in $[Q, Q_{SS}]$ are more diverse than for $[Q, C_{SS}]$. In humid regions, stable Q_{SS} could be sustained provided that there is sufficient river discharge even if C_{SS} fluctuates. In contrast, there is a decreasing trend in Q_{SS} in arid areas due to reduced Q , even when C_{SS} remains stable.

For the most commonly occurring $[Q, Q_{SS}]$ patterns, Fig. 4 describes river responses to different anthropogenic impacts in various climatic regions (mainly across the non-glaciered surface). A natural river basin with stable annual rainfall will retain stable trends in $[Q, Q_{SS}]$. When human activities occur, the $[Q, Q_{SS}]$ pattern of rivers in different climate zones will be altered in different ways. Activity A will make most rivers in humid regions exhibit Pattern II behavior, and Pattern V behavior

in arid regions. In contrast, Activity B will cause the majority of rivers in humid and arid regions to be characterized by Pattern III and Pattern IV behavior, respectively.

The trend in water flux affected by human activities must be fully considered. Soil and water conservation measures intercept precipitation, increase infiltration, and enhance evaporation, thereby decreasing Q [24]. Intensive water abstraction from rivers further reduces Q and thus modifies its trend [14]. Meanwhile, deforestation or the expansion of agriculture may lead to increasing Q [25].

Unlike ordinary rivers, an increased trend in river flux may occur in the relatively humid high-altitude Arctic river, such as the Yenisey River. This may be caused by increased runoff from rainfall or retreating glaciers responding to global warming [26, 27], but may also reflect measurement uncertainty [28].

3.3 Quantitative impacts of global climate change and human activities on trends in water and sediment fluxes

Quantitative evaluation has been made on the impacts of global climate change and typical human activities on changing trends in water and sediment fluxes in the world's large rivers. Significant correlation between water flux and precipitation ($P < 0.05$) is found in 71% (3050) of world's large rivers, whereas only 33% (101) of large rivers show significant correlation between sediment flux and precipitation. In Fig. 5a, precipitation explains over 80% of the changes in water flux [4] of large rivers located in northern Asia and northern Europe where impact of human activities is relatively limited. However, precipitation explains less than 30% of the variations in water flux of rivers in the mid-west of North America, eastern Africa, southern Africa, eastern Asia, and southeastern Asia experiencing large-scale dam construction and/or over-irrigation. On the other hand, precipitation variation explains less than 30% to the changes in sediment flux in most rivers globally, except for north of Asia, Europe,

and eastern North America (Fig. 5b). In contrast, less large rivers (23%) show significant correlations between temperature and water/sediment fluxes.

To distinguish human impacts from climate change, we used the Degree of Regulation Index (DOR, defined as the ratio of total storage capacity of all upstream dams to total discharge of the river, Fig. S1 online) related to dams, the Irrigation Index (defined as the ratio of irrigation area to virgin area contributing to the mean annual discharge, Fig. S2 online), precipitation, and temperature. Of the 1931 rivers with at least 40-year records, we find that higher DOR and Irrigation Index correspond to lower correlation between annual water discharge and precipitation/temperature, mainly in river basins where $DOR > 20$ and Irrigation Index > 140 (Fig. 5c). This suggests that changing trends in water flux in these areas are altered primarily by intensive human disturbance. Similarly, lower correlation ($P \geq 0.05$) between sediment flux and precipitation would be expected (Fig. 5d) upon $DOR > 8$ and irrigation index > 60 being met for concerned rivers. In general, sediment flux seems more sensitive to human interference than water flux in large rivers.

3.4 Water and sediment fluxes to the coastal ocean

We estimate that the total quantities of water flux Q and sediment flux Q_{ss} are 31,629 km³/a and 12,809 Mt/a respectively from global rivers to oceans based on new and previous [29] data on Q and Q_{ss} (1232 rivers for Q and 769 for Q_{ss}), using Milliman and Farnsworth's method [29] to determine post-dam Q_{ss} which takes account of regional change rate in sediment fluxes [30]. These results (Table S3 online) are very close to those obtained previously by Syed et al. [31] and Syvitski et al. [23, 32]. At continental scale, estimated values of annual Q and Q_{ss} are similar to those in other studies [17, 29, 31–35], except for the values of Q and Q_{ss} in Asia, Q in

Africa and Q_{SS} in Oceania (Table S3 online). These discrepancies arise because our updated data inherently take account of recent changes in Q and Q_{SS} in Asia, Q in Africa, and we consider high Q_{SS} values occurring in rivers located on ocean islands [29].

We have also assessed the total water and sediment fluxes from the land to oceans over the past 5–10 years, and compared it with the long-time average annual value. Based on the observed water flux in 828 large rivers discharging to the oceans, which represents 86% of the area of active water discharge [17], we find that Africa and Asia show significant decreases over the past 5–10 years when compared with the longer-term mean, while Eurasian Arctic and South America demonstrate increases. However, sediment flux to the sea declined significantly (by 1802–1909 Mt/a) in 193 large seaward rivers, representing 61% area of active water flux [17] (Table S4 online). Most of the reduction in land-ocean sediment flux occurs in Asian and African rivers, though small increases are found in Oceania and South America.

Carrying out a further extended study including smaller rivers in other 14%–39% of data-scarce active discharge areas, we estimate that the mean annual water and sediment fluxes to sea from the world's rivers decreased by 58–98 km³/a (0.25%) and 2617–2715 Mt/a (20.8%) respectively over the recent 5–10 five- to ten-year timescale, mainly due to the reduction in Q and Q_{SS} that occurred in Asia (by 1.6%–2.0% in Q , and by 13.1%–13.2% in Q_{SS}) and Africa (by 0.3%–0.4% in Q , and by 6.7%–6.8% in Q_{SS}). The similar regional change rates of Q and Q_{SS} obtained from 828 large seaward rivers are satisfactory approximations [30]. Looking at individual rivers it can be noted that the change in Q of the Amazon River, which contributes globally about 18% of Q to the sea, is relatively small (1.0%–0.9%). In contrast, Q_{SS} transported by the world's largest fluvial sediment carrier, the Yellow River, only

reached 11.3% of the 1950s level in the most recent decade, and its reduction from 1950s to 2000s accounts for 9.2% of global sediment flux to the oceans.

4. Conclusions

Based on the first exploration on the co-varying trends in water-sediment fluxes characterized with 9 typical binary patterns, we found that evolving patterns of change in the water and sediment fluxes of the world's large rivers are dominated by stationary behavior at the global scale, while 24% of the world's large rivers are experiencing significant changes in water flux and 40% in sediment flux. Furthermore, modification of the global hydrological cycle by climate change (in particular change of precipitation) and increased irrigation [36] are driving changes in water flux, while human activity may cause local decreases or increases in sediment flux through activity types A (in particular dam construction, irrigation and water-soil conservation) or B (notably deforestation, mining, and land clearance), respectively, thus altering the trends in Q_{SS} in different river basins. More recent change identified by this study is the marked decrease (20.8%) in the global land-ocean sediment flux that occurred in the recent five to ten years, mostly (13.2%) contributed by Asian rivers due to accelerated human disturbance of river basin sediment budgets particularly as a result of dam construction. The findings presented highlight the increasing significance of climate change and human impacts on the world's large rivers which upscale to cause changes in global river fluxes of water, sediment and associated materials, and important impacts on riverine, estuarine, coastal environments, and biogeochemical cycles.

Conflict of interest

The authors declare that they have no conflict of interest.

Acknowledgments

This work was supported by the National Natural Science Foundation of China (51721006 and 91647211).

Author Contributions

JR Ni and DE Walling designed the research. L Li, JR Ni and AGL Borthwick performed the research. L Li, F Chang and Y Yue conducted the data analysis. DE Walling, N Frolova, D Magritsky, P Ciais, Y Yue, YC Wang, and CM Zheng contributed new ideas and information; L Li, JR Ni, AGL Borthwick and DE Walling wrote the paper. All of the authors contributed to interpretation of the findings.

References.

1. Döll P, Zhang J. Impact of climate change on freshwater ecosystems: a global-scale analysis of ecologically relevant river flow alterations. *Hydrol Earth Syst Sci* 2010; 14: 783–799.
2. Xu BC, Yang DS, Burnett WC, et al. Artificial water sediment regulation scheme influences morphology, hydrodynamics and nutrient behavior in the Yellow River estuary. *J Hydrol* 2016; 539: 102–112.
3. Beechie TJ, Sear DA, Olden JD, et al. Process-based principles for restoring river ecosystems. *Bioscience* 2010; 60: 209–222.
4. Wang S, Fu BJ, Piao SL, et al. Reduced sediment transport in the Yellow River due to anthropogenic changes. *Nature Geosci* 2016; 9: 38–41.
5. Zhao YF, Zou XQ, Gao JH, et al. Quantifying the anthropogenic and climatic contributions to changes in water discharge and sediment load into the sea: A case study of the Yangtze River, China. *Sci Total Environ* 2015; 536: 803–812.

6. Syvitski JPM, Kettner AJ, Overeem I, et al. Sinking deltas due to human activities. *Nature Geosci* 2009; 2: 681–686.
7. Latrubesse EM, Arima EY, Dunne T, et al. Damming the rivers of the Amazon basin. *Nature* 2017; 546: 363–369.
- 5 8. Bégin C, Wurzbacher J, Côté IM. Variation in benthic communities of eastern Caribbean coral reefs in relation to surface sediment composition. *Mar Biol* 2013; 160: 343–353.
9. Chen YS, Zhang SH, Huang DS, et al. The development of China's Yangtze River Economic Belt: how to make it in a green way? *Sci Bull* 2017; 62: 648–651.
- 10 10. Wang HJ, Saito Y, Zhang Y, et al. Recent changes of sediment flux to the western Pacific Ocean from major rivers in East and Southeast Asia. *Earth-Sci Rev* 2011; 108: 80–100.
11. Bobrovitskaya NN, Kokorev AV, Lemesko NA. Regional patterns in recent trends in sediment yields of Eurasian and Siberian rivers. *Global Planet Change* 2003; 39: 127–146.
- 15 12. Walling DE. Human impact on land–ocean sediment transfer by the world's rivers. *Geomorphology* 2006; 79: 192–216.
13. Walling DE, Fang D. Recent trends in the suspended sediment loads of the world's rivers. *Global Planet Change* 2003; 39: 111–126.
- 20 14. Milliman JD, Farnsworth KL, Jones PD, et al. Climatic and anthropogenic factors affecting river discharge to the global ocean, 1951–2000. *Global Planet Change* 2008; 62: 187–194.
15. Dai A, Qian TT, Trenberth KE, et al. Changes in continental freshwater discharge from 1948 to 2004. *J Climate* 2009; 22: 2773–2792.

16. Ruoppa M, Karttunen K. Typology and ecological classification of lakes and rivers. Copenhagen: Nordic Council of Ministers; 2002.
17. Fekete BM, Vörösmarty CJ, Grabs W. High-resolution fields of global runoff combining observed river discharge and simulated water balances. *Global Biogeochem Cycles* 2002; 16: 15-1–15-10.
18. Runkel RL, Crawford CG, Cohn TA. Load Estimator (LOADEST): a FORTRAN program for estimating constituent loads in streams and rivers. <https://pubs.usgs.gov/tm/2005/tm4A5/pdf/508final.pdf>.
19. Duan W, Takara K, He B, et al. Spatial and temporal trends in estimates of nutrient and suspended sediment loads in the Ishikari River, Japan, 1985 to 2010. *Sci Total Environ* 2013; 461: 499–508.
20. Mann HB. Nonparametric tests against trend. *Econometrica* 1945; 13: 245–259.
21. Kendall MG. Rank correlation methods. Glasgow: Charles Griffin and Company Limited; 1948.
22. Yue S, Pilon P, Phinney B, et al. The influence of autocorrelation on the ability to detect trend in hydrological series. *Hydrol Process* 2002; 16: 1807–1829.
23. Syvitski JPM, Vörösmarty CJ, Kettner AJ, et al. Impact of humans on the flux of terrestrial sediment to the global coastal ocean. *Science* 2005; 308: 376–380.
24. Miao CY, Ni JR, Borthwick AGL, et al. A preliminary estimate of human and natural contributions to the changes in water discharge and sediment load in the Yellow River. *Global Planet Change* 2011; 76: 196–205.
25. Gebremicael TG, Mohamed YA, Betrie GD, et al. Trend analysis of runoff and sediment fluxes in the Upper Blue Nile basin: a combined analysis of statistical tests, physically-based models and landuse maps. *J Hydrol* 2013; 482: 57–68.

26. Shiklomanov AI, Lammers RB. River ice responses to a warming Arctic—recent evidence from Russian rivers. *Environ Res Lett* 2014; 9: 035008.
27. Ding YJ, Zhang SQ, Zhao L, et al. Global warming weakening the inherent stability of glaciers and permafrost. *Sci Bull* 2019; 64: 245–253.
- 5 28. Shiklomanov AI, Yakovleva TI, Lammers RB, et al. Cold region river discharge uncertainty—estimates from large Russian rivers. *J Hydrol* 2006; 326: 231–256.
29. Milliman JD, Farnsworth KL. River discharge to the coastal ocean: a global synthesis. New York: Cambridge University Press; 2011.
30. Liu C, Hu CH, Ye H. Total sediment flux entering the sea from major Chinese rivers and rough estimation for global land-ocean sediment flux. In: Fukuoka, S, Nakagawa, H, Sumi, T et al (ed.). *Advances In river sediment research*. London: CRC; 2011.
- 10 31. Syed TH, Famiglietti JS, Chambers DP. GRACE-based estimates of terrestrial freshwater discharge from basin to continental scales. *J Hydrometeorol* 2009; 10: 22–40.
- 15 32. Syvitsk JPM, Kettner A. Sediment flux and the anthropocene. *Phil Trans R Soc A* 2011; 369: 957–975.
33. Baumgartner A, Reichel E. Mean annual global: continental and maritime precipitation, evaporation and run-off. Amsterdam: Elsevier; 1975.
- 20 34. Holeman JN. The sediment yield of major rivers of the world. *Water Resour Res* 1968; 4: 737–747.
35. Milliman JD, Meade RH. World-wide delivery of river sediment to the oceans. *J Geol* 1983; 91: 1–21.
36. Oki T, Kanae TS. Global hydrological cycles and world water resources. *Science* 25 2006; 313: 1068–1072.

Figure Captions.

Fig. 1. Trends in water discharge Q for 8089 hydrologic stations located in 4307 of the world's large rivers, and suspended sediment concentration C_{SS} and suspended sediment flux Q_{SS} for 496 stations on the 309 large rivers color coded according to basin climate conditions and bounded by dashed lines (left plots); and global spatial distributions of trends in Q , C_{SS} and Q_{SS} (right panels). (a) Q . (b) C_{SS} . (c) Q_{SS} . All trends are significant at the 0.05 level.

Fig. 2. Nine basic $[Q, Q_{SS}]$ patterns. (a) Matrix of nine pattern representing the changes of $[Q, Q_{SS}]$. (b) representative large rivers for nine different $[Q, Q_{SS}]$ patterns showing water flux (solid line) and sediment flux (histogram) time histories and corresponding trends (dashed line): (1) Rhine River at Rhenish Massif, (2) Yangtze River at Datong, (3) Amazon River at Obidos, (4) Songhuajiang at Jiamusi, (5) Yellow River at Lijin, (6) Nenjiang at Jiangqiao, (7) Yana River at Ubileynaya, (8) Mississippi River at Tarbert Landing, and (9) Blue Nile River at El Diem. All trends are significant at the 0.05 level.

Fig. 3. Asian rivers' contribution on $[Q, Q_{SS}]$ trends for world's large rivers over past decade and comparison of observed and estimated prehuman sediment fluxes. (a) River numbers according to $[Q, Q_{SS}]$ patterns, with and without Asian rivers. (b) Comparison between pre-human and observed Q_{SS} ; the Asian rivers' names are: 1, Amguema; 2, Kolyma; 3, Alazeya; 4, Yana; 5, Lena; 6, Anabar; 7, Yenisei; 8, Taz; 9, Ob; 10, Indus; 11, Ganges; 12, Chao-Phraya; 13, Mekong; 14, Zhujiang; 15, Yangtze;

16, Minjiang; 17, Qiantangjiang; 18, Huaihe; 19, Yellow; 20, Haihe; 21, Liaohe; 22, Xiaolinghe; 23, Yalujiang; 24, Sakarya. (c) Rivers' number percentage according to $[Q, Q_{ss}]$ patterns, with trends determined for two periods. (d) omparison between pre-human and observed Q_{ss} ; the river names are: 1, Lena; 2, Yenisei; 3, Ob; 4, Severnaya-Dvina; 5, Danube; 6, Rhine; 7, Ebro; 8, Nile; 9, Kuban; 10, Indus; 11, Chao-Phraya; 12, Mekong; 13, Zhujiang; 14, Yangtze; 15, Minjiang; 16, Qiantangjiang; 17, Huaihe; 18, Yellow; 19, Xiaolinghe; 20, Liaohe; 21, Yalujiang; 22, Fitzroy; 23, Kenai; 24, San-Joaquin; 25, Mississippi; 26, Hudson; 27, Rio-Grande; 28, Amazon; 29, Parana; 30, Elqui; 31, Itata; 32, Biobio. Colored areas in inset-maps in b and d denote large river basins.

Fig. 4. The impact of two types of human activities on the most commonly occurring $[Q, Q_{ss}]$ trends under different climatic conditions.

Fig. 5. Impacts of climate change and varying human activities on changing trends in water and sediment fluxes of global large rivers. (a) Contribution of precipitation variation to change in water discharge in large rivers ($P < 0.05$). (b) Contribution of precipitation variation to change in sediment flux in large rivers ($P < 0.05$). (c) DOR and Irrigation Index in the 1931 rivers with > 40 -year records of water discharge (0 are plotted as 0.01). (d) DOR and Irrigation Index in the 74 rivers with > 40 -year records of sediment flux (0 are plotted as 0.01).

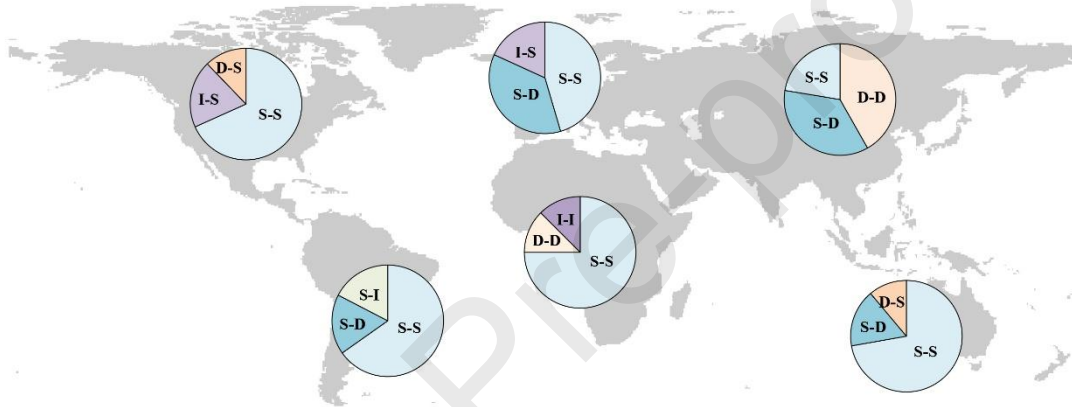
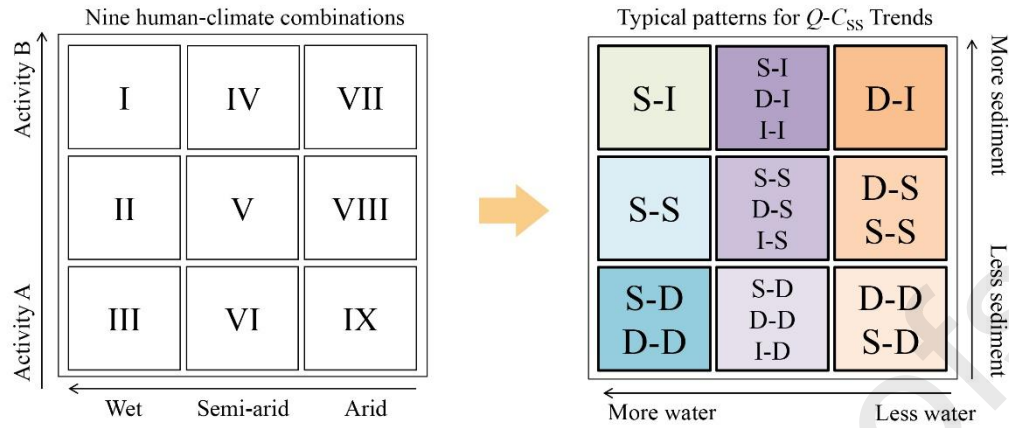


Li Li worked in Tianjin Institute of Water Transportation Engineering, Ministry of Transport. She received her B.Eng in Port Channel and Coastal Engineering from Wuhan University in 2012 and
5 Ph.D. in Environmental Engineering at Peking University in 2017. Her work focuses on water and sediment transport in rivers.

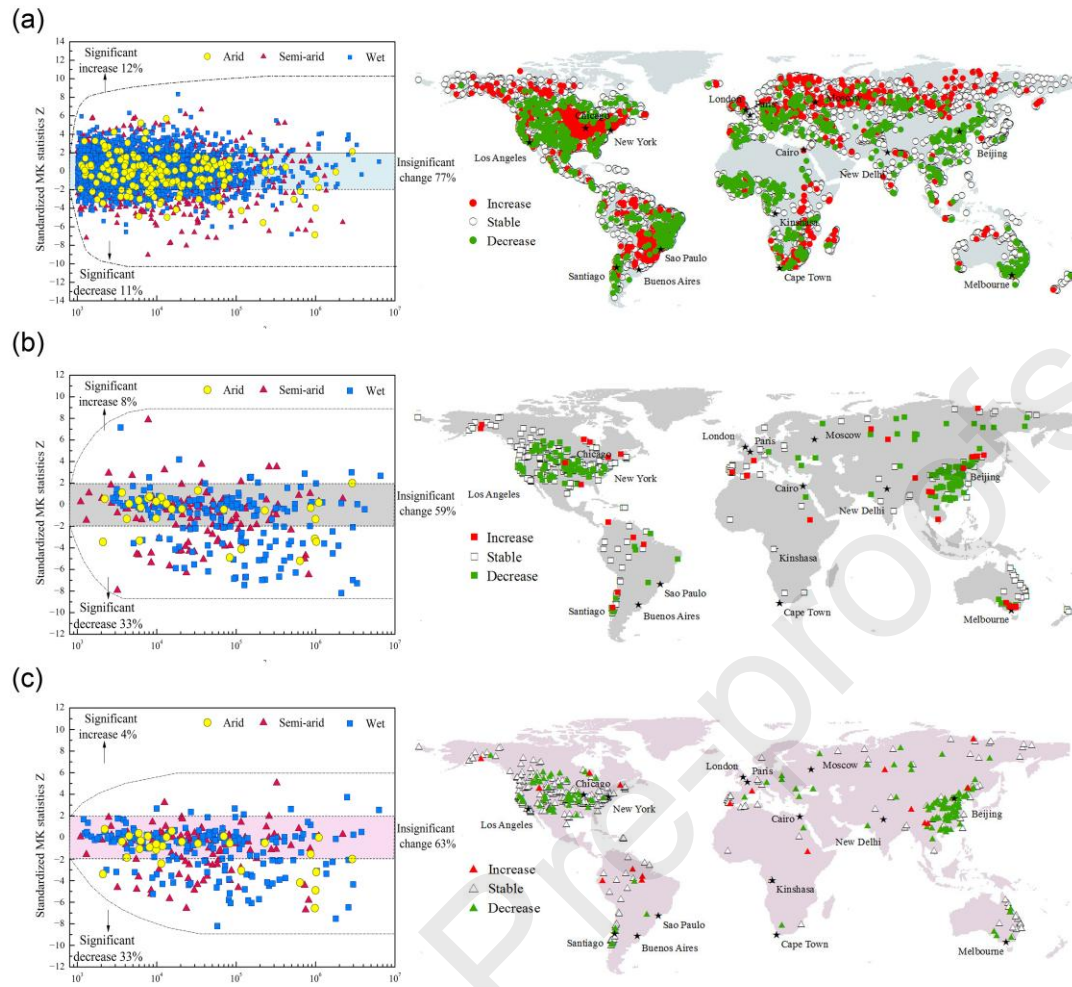


10 Jinren Ni is currently a professor at Department of Environmental Engineering at Peking University. He graduated in Port Channel and Coastal Engineering from Wuhan University in 1982, received M.Sc and Ph.D. in River and Coastal Dynamics and Hydraulics at Tsinghua University in 1985 and 1989, respectively. His work focuses material fluxes in aquatic ecosystems and river sustainability.

15



Graphic Abstract. Combinations of climatic zones and human activities (A and B denote types of conservation and exploitation activities respectively) well correspond to the nine water-sediment co-varying trends (S, D, and I represent stable, decrease and increase trends respectively) in the world's large rivers distributed globally.



(a)

Q_{ss} \ Q	Q		
	Stable	Decrease	Increase
Stable	Pattern I S-S	Pattern IV D-S	Pattern VII I-S
Decrease	Pattern II S-D	Pattern V D-D	Pattern VIII I-D
Increase	Pattern III S-I	Pattern VI D-I	Pattern IX I-I

(b)

